

## Lidar-backscattered signal modulation and design for a specific emitting module

Zhang Xiaofu, Le Xiaoyun

(School of Physics and Nuclear Energy Engineering, Beihang University, Beijing 100191, China)

**Abstract:** The cloud lidar, with the character of high precision and good stability, is an effective way to detect the cloud height. Pulse diode laser (PLD), as an essential part of the lidar system, needs the triggering pulse. In this paper, the emitting part of the lidar was studied, including the simulation of the backscatter SNR, choosing of PLD and design of triggering circuit to drive the 905 nm PLD with the consideration of the optical system. A circuit for triggering the laser pulse with adjustable power and pulse width was contrived. Then the software Systemview was used to emulate the design and finally the making of PCB was finished. The results show whatever the parameters of the pulse, namely triggering pulse width, the rising edge, dithering, all these can be qualified to be in use in practice and enjoys the merits of low cost and convenience. The emitting module operates well.

**Key words:** lidar; pulse diode laser; backscatter SNR; triggering circuit

**CLC number:** TN958.1    **Document code:** A    **Article ID:** 1007-2276(2015)03-0888-05

## 对激光雷达特定的发射模块后向散射信号的调制和设计

张小富,乐小云

(北京航空航天大学 物理科学与核能工程学院, 北京 100191)

**摘要:** 测云激光雷达具有精度高和稳定性好的特点,是检测云高的有效途径。作为激光雷达系统的一个基本组成部分,脉冲二极管激光器(PLD)需要脉冲信号触发。对激光雷达的发射部分进行了研究,其中包括后向散射信噪比的仿真、脉冲二极管激光器的选择与触发电路、用于驱动综合光学系统的波长为 905 nm 的 PLD 的电路。触发电路激光脉冲具有可调功率和脉冲宽度功能。用 Systemview 软件仿真设计,完成了 PCB 版的制作。结果表明:脉冲的任何参数即触发脉冲宽度、上升沿、抖动等均可用于实验中,并具有低成本和使用方便的优点。该发光模块在测云激光雷达中运行良好。

**关键词:** 激光雷达; 脉冲半导体激光器; 后向散射信噪比; 触发电路

## 0 Introduction

Cloud lidar is a new method based on principles of cloud detection lidar and atmospheric scattering theory. Compared to other measurement techniques such as cloud height measurement ceiling projector, rotating beam Cloud lidar cloud height measurement method, balloon testing cloud height method, cloud lidar has its unique advantages of wide measuring range, high accuracy and good stability. In addition, important atmospheric parameters such as vertical visibility, cloud height and cloud base and backscattering profiles could be obtained after the certain inversion algorithm for the aerosol or cloud backscattered signals. Thus the cloud lidar has been widely used in airports, launching sites, meteorological stations, air pollution monitoring campaign and other fields.

## 1 Lidar equation

The lidar equation relating the backscattering signal is given as:

$$P_r(R) = K\beta(R)\exp\left[-2\int_0^R \alpha(r)dr\right] / R^2 \quad (1)$$

Where  $P_r(R)$  is the backscattering signal power;  $K$  is the system constant;  $\beta(R)$  is the backscattering coefficient, and  $\alpha(r)$  is the extinction coefficient, where  $\alpha(r) = s(r) + a(r)$ ,  $s(r)$  and  $a(r)$  are scattering and absorption coefficients of a particle respectively. The system constant  $K$  consists of the product of the laser emitting power  $P_0$ , optical efficiency of the receiving optics, receiving area  $A_r$ , and the half of the pulse spatial width  $l$ ,  $l = c/2$ , where  $c$  is the light velocity and is the pulse temporal width). In Eq.1, the quantities of  $\beta(R)$  and  $\alpha(r)$  are two unknown quantities. Usually, both  $\beta(R)$  and  $\alpha(r)$  consist of contributions from both air molecules and particulates. The lidar equation has the analytical solution when we have a simple relation between  $\beta(R)$  and  $\alpha(r)$ . Theoretically for the coaxial laser radar, as long as the receiver FOV is larger than the laser beam divergence angle, the

overlap factor can be considered as always 1. However, in order to avoid saturation problems in practical use, an aperture is often used to control the backlight.

## 2 Selection for laser and SNR simulation

In the laser remote sensing technology, semiconductor laser diodes are usually used as signal source and low noise avalanche diode (Si APD) as the detector. Compared with other lasers, semiconductor laser diode with the merits of small size, long life, variety, high efficiency, and convenience use, has become the widely used laser in the pulsed laser measurement<sup>[1-4]</sup>. When selecting the laser, firstly the laser wavelength and the emission energy is considered. For various clouds, cloud droplet radius usually ranges between 1–100  $\mu\text{m}$ , which most of the radius are between 2–15  $\mu\text{m}$ . Based on the Mie scattering theory  $2\pi r/\lambda \gg 1$ , the wavelength should be less than 1  $\mu\text{m}$ . Taking into account several weak absorption bands of the atmosphere, the laser wavelength should be selected in the 800–1000 nm window atmosphere, optionally in the value of about 900 nm. Currently the available emission wavelength is 905 nm.

There is a direct relationship between the laser transmitter and receiver devices, so in order to explore requirements of the detection laser energy, the atmospheric echo signal to noise ratio (SNR) of laser equations must be simulated. Usually the low noise Si-APD detectors<sup>[5]</sup> are mostly used in near-infrared laser detection. The equation of SNR is described as follow<sup>[6]</sup>:

$$SNR = \left( \frac{AT_r k_0}{4e\Delta f} \right)^{\frac{1}{2}} \frac{E_0 c \eta(R) r^2 \beta(r) \exp\{-2\int_0^r \alpha(r')dr'\}}{\sqrt{E_0 c \eta(R) r^2 \beta(r) \exp\{-2\int_0^r \alpha(r')dr'\} + 2P_{\text{back}} \pi \left(\frac{\theta_r}{2}\right)^2 \lambda_r}} \quad (2)$$

Laser radar parameters used in the simulation are shown in Tab.1, the atmospheric model is in

reference[7] and [8]. In aim to study the impact of the laser emission power and the frequency on the cloud properties, several calculations were carried out. Figure 1 shows the backscatter SNR for different emitting power, and we can see the higher the energy, the higher the SNR becomes. Figure 2 shows the SNR profile with the different pulse energy and frequencies.

**Tab.1 Parameters to simulate the backscatter SNR of the lidar**

Model	Si
Active area $A$	$0.5 \text{ mm}^2$
Optical transmittance $T_r$	60%
Responsibility $k_0$	$1 \times 10^6 \text{ V} \cdot \text{W}^{-1}$
Amplifying bandwidth $\Delta f$	30 M
Field view $\theta_r$	1.6 mrad
$P_{\text{back}}$	$0.8 \text{ Wm}^{-1} \cdot \text{nm}^{-1} \cdot \text{sr}^{-1}$
$\text{FWHM} \cdot \lambda_r$	10 nm

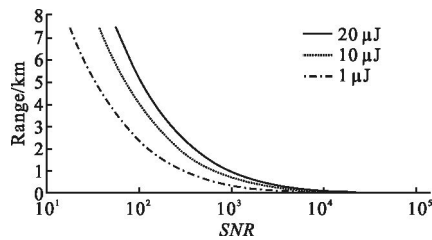


Fig.1 Comparison of the backscatter SNR for different emitting power

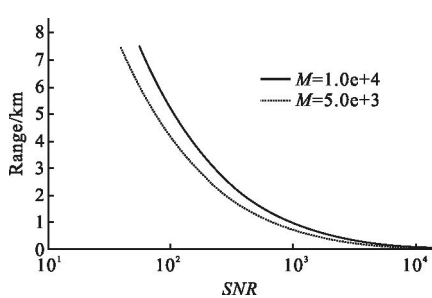


Fig.2 Comparison for different emitting pulse numbers

### 3 Emission model design

Parameters used in the semiconductor laser 905 nm laser radar system is as follows: peak power is 40–220 W (adjustable), pulse width is 30–100 ns (adjustable) with the range of pulse energy between 1.2–22  $\mu\text{J}$  (adjustable). The maximum average power of 110 mW requires TTL rising edge trigger, 5 kHz of

repetition frequency, and duty cycle of 0.05%<sup>[9–10]</sup>. If 20 M crystal is utilized to produce 5 kHz frequency, time delay is needed. The trigger pulse duty cycle should be 0.05% and the pulse width is 100 ns. Pulse laser transmitter module design must take into account the constraining relationship between the laser emission frequency and transmitting power. Since the transmitting power of the laser diode is fixed, the emitted power will be reduced as the repetition frequency increases. The potential of diode laser could be maximized and came to the best use with the excellent driving pulse source. In the synchronous counter, the common clock, usually the input clock is used in every flip-flop. The flip-flop changes states synchronously and the counting speed is very fast. In the implementation a 20 M crystal, a D flip-flop, two synchronous counter 74HC40103B and finally a Schmitt trigger shaping are utilized.

74HC40103B is a CMOS high-speed 8-bit synchronous down counter. When (CI / CE) is at the high level, the counting cut off; The counter initial value is set as 4000 with the binary value of 111 110 011 111, and it requires two cascading counters. Firstly the synchronous working end and the asynchronous resetting end were set at the high level. After a rising pulse comes along, subtraction counter operated. Then when the output is zero, a pulse was produced after a wave shaper. The specific realizing steps of dynamic creating forms are set forth. 20 M crystal was passing through four D flip-flops with 16 points dividing frequency. The output, as the main frequency clock signal was sent to the first piece of 74HC40103B. At the same time, the clock signal was sent to the second the clock pulse rising along the 74HC40103B scored the second piece of 74HC40103B after the two Schmitt triggers. When the rising edge of pulse arrived, the first piece of synchronous counter chip produced the high and the subtraction counter began to decline. During this period, this process has always been to high level. When the first piece of counter counted to zero, the low level was come out. Next the

low level was served as a starting signal to the second counter. So when the counter decreased to zero again, the signal was sent to the synchronous working end until the next synchronous clock arrived. Until then the pulse signal output began a new cycle. The trailing edge of the pulse signal will be captured by the detection unit, which was composed of 2D flip-flops. Furthermore a pulse width was produced after the falling edge of the pulse signal. Finally the waveform was output through the Schmitt trigger SN74HC14N.

### 4 Results

Figure 3 and Figure 4 illustrates the simulation design and result from software systemview. In the latter circuit design, double-sided PCB was used in the circuit board with one for circuit wiring, another for components. The components of the whole surface are made of ground copper foil, making less earth resistance and inductance. And the basic electronic potential between the grounds were equal. Because the entire circuit elements were close to the "ground", some interfering electric fields were thus directly

accessed to "ground". It has weakened the crosstalk between lines and components and effectively eliminated the pulse crosstalk. According to the size of the printed circuit board current, the power line width was overstriking as possible to reduce the loop resistance. The circuit diagram and eventually the triggering results are shown in Fig.5 and Fig.6.

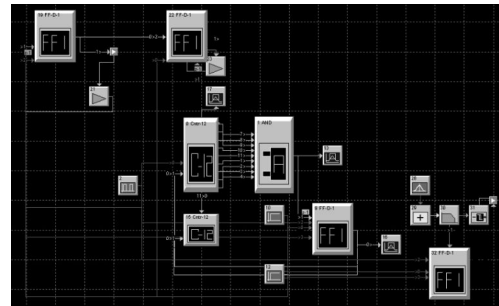


Fig.3 Emulation of the circuit with Systemview

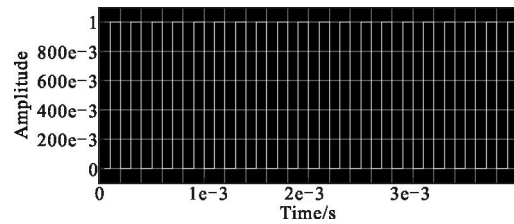


Fig.4 Results of the emulation

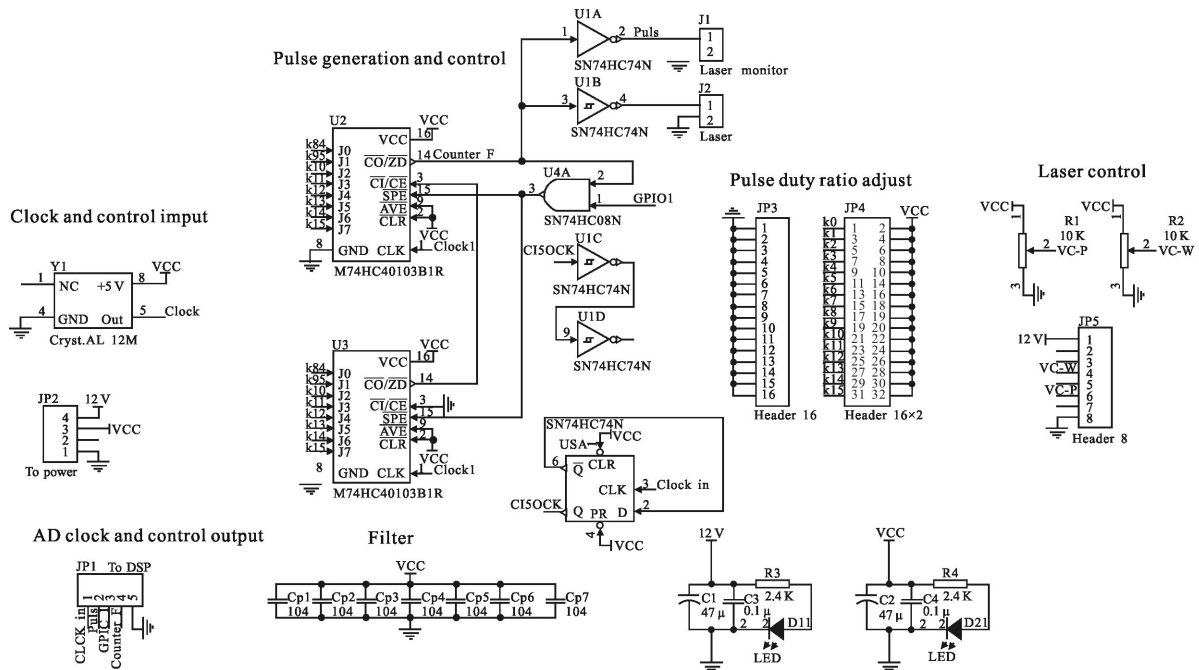


Fig.5 Hardware principle of the circuit

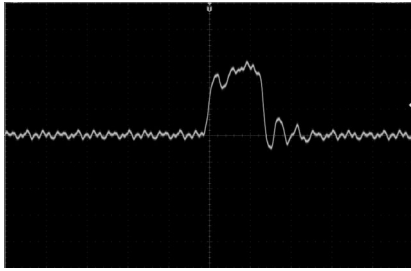


Fig.6 Experimental results of the triggering signal

## 5 Conclusion

In this paper the cloud lidar launching module is studied assuming the certain simulating parameters and the atmospheric model. According to the signal to noise ratio equation, the appropriate laser beam power is calculated. And the emitting laser model is used considering several performance parameters such as wavelength and output pulse rising time. Then the feasible digital logic circuit is designed to obtain the one over four thousand of the duty ratio for the triggering clock. Finally the experimental data imply that the optical pulse can satisfy the demand of the system.

## References:

- [1] Shiv R Pal, Wolfgang Steinbrecht, Allan Carswell. Automated method for lidar determination of cloud-base height and vertical extent[J]. *Appl Opt*, 1992, 31: 1488-1494.
- [2] Cross P S, Harnagel G L, Streifer W, et al. Ultra high-power semiconductor diode laser arrays [J]. *Science*, 1987, 237 (4820): 1305-1309.
- [3] Chan K. Generation of high-power nanosecond pulses from laser diode-pumped Nd:YAG lasers [J]. *Appl Opt*, 1988, 27(7): 1227-1230.
- [4] Chan K. Multiple-pass laser-diode-pumped Nd:YAG amplifier: design [J]. *Apply Opt*, 1987, 26 (6): 3177-3179.
- [5] Guo Shujun, Li Shukai. The detection of the laser pulse signal with a Si-APD[J]. *Chinese Laser*, 2002: 29(6): 121-127. (in Chinese)
- [6] Huang Wuhan. Laser Communication and Lidar Technology [M]. Beijing: Posts and Telecom Press, 1999. (in Chinese)
- [7] Fernald F G. Analysis of atmospheric lidar observation :some comments[J]. *App Opt*, 1984, 23(5): 652-653.
- [8] Elske V P Smith, David M Gottlieb. Solar flux and its variations[J]. *Space Science Reviews*, 1974, 16(5-6): 771-802.
- [9] Wang Wenli, Shang Zhixin. Design of high performance pulse signal generator based on CPLD [J]. *Foreign Electronics*, 2007, 9(7): 65-68.
- [10] Bao Daoye. The Design and the Application of the Oscillating Circuit[M]. Beijing: Science Press, 2005: 59-60. (in Chinese)